

ENGINEERING DESIGN USING EVOLUTIONARY STRUCTURAL OPTIMISATION BASED ON ISO-STRESS-DRIVEN SMOOTH GEOMETRY REMOVAL

M.J. García*, **O.E. Ruiz[†]** and **G.P. Steven[‡]**

Mechanical Eng Dept. EAFIT University, Medellin, Colombia

School of Engineering University of Durham, UK

Abstract.

The main goal of Evolutionary Structural Optimisation (ESO) research has been to provide an easily applicable optimisation method for the engineering industry which assists the design process for product improvement. Originally ESO was based on the concept of fully stressed structures and it is obtained by slowly removing, from a Finite Element mesh these elements that present the lowest stress value. Following this heuristically-driven removal criteria, the initial topology evolves towards the optimum one. Since its introduction in 1992, ESO has been developed and extended to several types of structural problems. Initial weaknesses of ESO were (i) typically long solution times and (ii) topologies with jagged surfaces as a result of removing whole elements in the optimisation process. These characteristics hindered its application to computer aided design and analysis. In this investigation, these weaknesses have been addressed for 2D situations by (i) basing the stress computation on the Fixed Grid (FG) finite element method and (ii) removing material with the lowest values along iso-stress contours instead of removing whole elements. A boundary representation (B-rep) of the structure is maintained at each iteration of the optimisation process. Modification to the workpiece is made by identifying the stress contour lines and incorporating them into the evolving geometry. The topological consistency of the B-rep is maintained via normalized 2D boolean operations.

*Computational Mechanics Group, EAFIT University

[†]CAD/CAM/CG Group, EAFIT University

[‡]Professor of Engineering, University of Durham

element domain. This process is known as the mesh generation process and usually requires large computational resources.

By way of contrast, a Fixed Grid (FG method) is generated by superimposing a rectangular grid of equal sized elements on the given structure instead of generating a mesh to fit the structure. Some of these elements are inside the structure (I), some are outside (O) and some are on the boundary, namely Neither-In-nor-Out elements (NIO) as illustrated in Fig. 1 [1]. An O element is given a material property significantly less than an I element and the problem becomes a bimaterial one. A NIO element is partially inside the structure and its material property value is not constant nor continuous over the element. Such an element is approximated by transforming the bimaterial element into a homogeneous isotropic element. The material property matrix of a NIO element is computed using Equation 1.

$$C^e(NIO) = \xi C^e(I) \quad (1)$$

where $C^e(NIO)$ is the elemental material property of a NIO element, $C^e(I)$ is the elemental material property of inside, $\xi = A_I/A_e$ is the area ratio of the area inside of the structure within the NIO element A_I , over the total area of an element A_e .

1.2 Evolutionary Structural Optimisation (ESO).

Evolutionary Structural Optimisation method is based on the concept that by removing inefficient material from a structure its residual shape evolves in the direction of a better one. As such, it uses numerical solvers (among them FG). In its classic form ESO method optimises a structure by slowly removing *elements* with low stress, approaching a fully stressed design [3]. An important characteristic of the ESO method is that it is easy to understand and learn while at the same time produces reliable results. Hence ESO has been extended to accommodate various optimisation criteria and is becoming a more practical method. Some of these developments include the implementation of stiffness and displacements as optimisation criteria [4] and the applications in multiple load [5], non-linear [6], dynamic [7] and buckling problems [8]. Querin et al. extended the ESO method to add as well as remove elements, namely Bi-directional ESO (BESO) [9]. This meant that the initial design no longer had to be the maximum design domain. Thus, the solution time may be reduced especially if the user specifies a near-optimal topology as the initial design. However this knowledge is not always available and the typical long solution time of ESO has been an obstacle against its practical applicability as a design tool

1.2.1 Classic Evolutionary Structural Optimisation (ESO)

The basic concept of the stress-based Classic ESO is that a structure evolves towards a fully stressed design, ie. an optimum, by slowly removing the lightly stressed elements. The elements that satisfy the ESO inequality of Equation (2) are not being efficiently utilised in carrying the applied load and hence can be removed with a minimal effect on the structural integrity. The ESO procedure can be summarized as presented in Algorithm 1.

$$\sigma_{vm}|_e \leq RR \times \max(\sigma_{vm}) \quad (2)$$

$$RR = a_0 + a_1 \times SS + a_2 \times SS^2 + a_3 \times SS^3 + K \quad (3)$$

where

$\sigma_{vm} _e$	=	Average von Mises stress at element e ,
$\max(\sigma_{vm})$	=	maximum von Mises stress of the structure,
RR	=	Rejection Ratio,
a_0, a_1, a_2, a_3	=	user specified constants that define the rate at which the elements are removed, and
SS	=	Steady State number, [4].

Algorithm 1 Main ESO algorithm

```
while optimum limit is not reached do  
  Carry out FEA;  
  Remove elements according to Equation (2) ;  
  if number of removed elements == 0 then  
     $SS = SS + 1$ ;  
  end if  
end while
```

1.2.2 Fixed Grid Evolutionary Structural Optimisation (FG-ESO)

Kim et al [10] implemented FG into ESO. The main characteristic of FG-ESO is that elements are partially removed by modifying the ξ parameter in Equation (1). ξ represents the ratio of material inside the structure within an *NIO* element. They also propose a method for extracting the geometry of *NIO* elements from ξ parameters thus obtaining a smooth boundary representation of the optimal topology. The primary advantage of FG-ESO is a significant reduction in solution time. The FG uses *NIO* elements, which represent a fraction of the area of a nominal cell. The application of these elements in ESO enabled a more refined optimisation than the traditional ESO method for the same mesh density. It is also noted here that the optimal topologies do not contain checkerboard patterns, and therefore are more feasible and manufacturable relative to

typical optimised topologies [11, 12]. In this approach the physical realization of the workpiece is achieved by back-translating cells with $0.0 \leq \xi \leq 1.0$ into patterns of predefined fractions of square regions.

1.2.3 Scope of present study

In ESO method the structure is optimised by slowly removing inefficient material which is accomplished by removing elements with low average stress as in Equation (2). In this study, the “inefficient material” is identified by the contour lines at $\sigma_t = RR \times \max(\sigma_{vm})$. Then the B-rep of the structure is modified by subtracting the material defined by these contour lines. Finally, topological and mechanical consistency of the B-rep is maintained by a continuous assessment of these evolving geometries. In this approach the boundaries of the subtracted regions do not have to be aligned with the orthogonal grid (Orthogonality Constraint is removed). The method itself is independent on the analysis method since the information for material removal is concentrated on the iso stress curves. However, FG has been used because of its speed and re-analysis capabilities.

2 METHODOLOGY

Given the central role of boolean operations on 1-topological manifolds in the implementation of the ESO, a short review of relevant terms follows. A topological 1-manifold embedded in R^2 is a set $\Gamma \subset R^2$ such that $\forall p \in \Gamma, \exists U \subset R^2, U$ open, s.t. $p \in U, M \cap U$ is homeomorphic to R^1 . The boundary Γ of a 2D object is considered as being a *topological* 1-manifold. Being a topological manifold allows the boundary to be piecewise linear (PL). Homeomorphism forces it to be continuous. The *domain* of the Finite Element, Ω , is the closure of the interior of Γ . That means it is formed by the points enclosed by Γ and Γ itself. Notice that a convention is required since Γ divides R^2 into two disconnected regions, both of which could be considered as the finite element domain. The Boundary-representation of Ω is Γ , with the convention that it must be traversed in counter clockwise direction according to a vector normal to R^2 , in which Γ is embedded. Ω and Γ do not have to be connected sets from the topological point of view. They may represent (and enclose) disconnected portions of the piece. The mechanical stability of such a physical arrangement must be addressed outside of the topological considerations.

Figure 2 shows the main steps in implementing an ESO strategy on fixed grids using a piecewise linear contour. As a conclusion from the literature survey, one of the goals of this investigation is the computation and maintenance of a boundary that is not orthogonal (is not coincident with the grid). The boundary is allowed to cross grid elements with 1st degree (linear) curves.

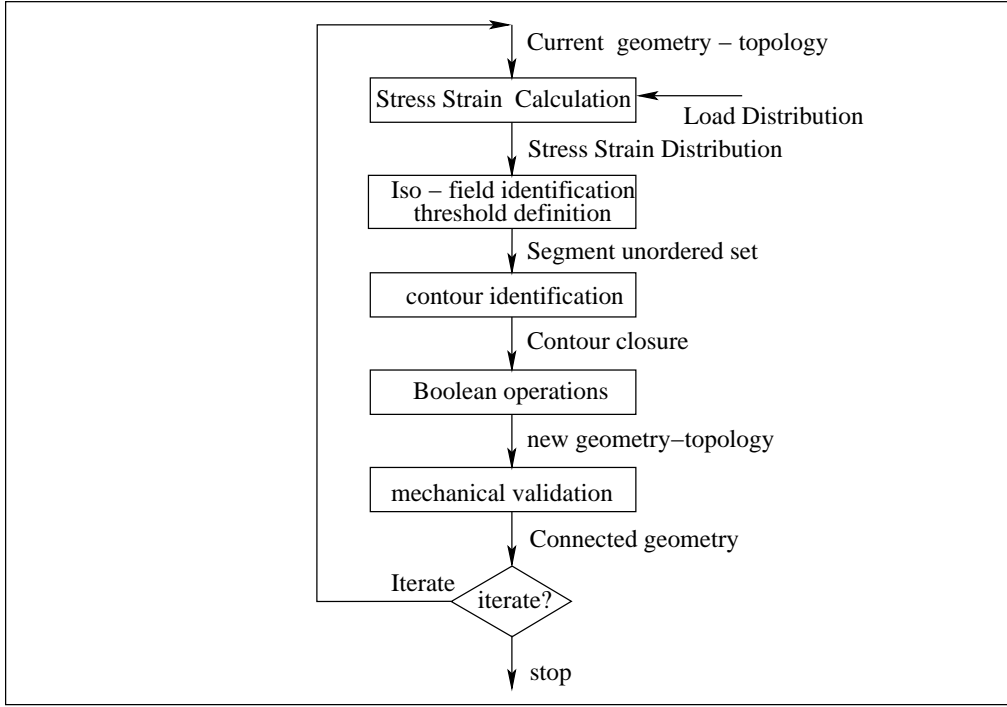


Figure 2: Main Algorithm for Non-Orthogonal Boundary Maintenance

The invariant of the algorithm is the existence of a valid boundary Γ_i in the i_{th} iteration. A valid boundary is (a) topologically consistent, (b) geometrically consistent, and (c) mechanically supported.

2.1 Fixed Grid without Orthogonality Constraint

Figure 3 shows the general configuration for iso-field curves intersecting the fixed grid. The approximation of the scalar field is of the form:

$$u(x, y) = \sum u_i \Phi_i(x, y) \text{ with } x, y \in \Omega \quad (4)$$

where $u_i = u(x_i, y_i)$ and $\Phi_i(x, y)$ is an element of the base function for the approximation space. The $\Phi_i(x, y)$ are defined by Lagrange polynomials of the form (i) $\Phi_i(x, y) = ax + by + cxy + d$ for a 4-node quadrangular element, and (ii) $\Phi_i(x, y) = ax^2y + bxy^2 + cx^2 + dy^2 + ex + fy + gxy + h$ for an 8-node quadrangular element. Parameter values in (i) or (ii) such as $a, b, etc.$ are obtained by evaluation of the scalar field $u(x, y)$ at the discrete corners dictated by the grid. For the set of base functions used here Equation (4) is non-linear. Its iso-values, dictated by $u(x, y) = u_0$ (or $du(x, y) = 0$) may intersect each limit of a given cell of the Fixed Grid in *two* points instead of one. Figure 3 displays the forms of the intersections of iso-stress displacement curves with a particular cell of the fixed grid.

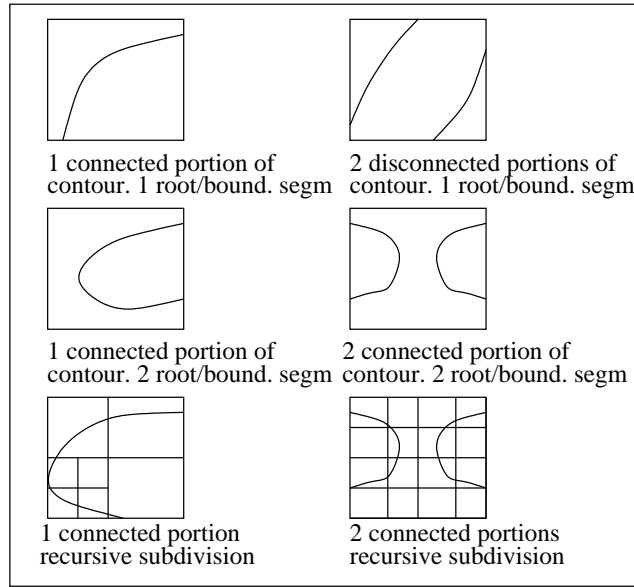


Figure 3: Configuration of Displacement Field Iso-stress within Fixed Grid Cells

2.2 Contour Identification

The identification of the iso-stress loci renders a set of unordered slightly curved segments. On each one the value of the function $u(x, y)$ is constant. However, the contour is approached by a Piecewise Linear (PL) path. This information is a (random) sample of the contour. Therefore, an additional algorithm is required to recover the connected, topologically correct PL contours Γ_i from the sampled data. The conditions that must be met are: (i) Γ_i must be closed. (ii) Γ_i must be traversed in CCW direction according to the normal vector of the 2D space embedding Γ_i . (iii) $\Gamma_i \cap \Gamma_j = \Phi$ $i \neq j$. Contours do not touch each other. (iv) $\Gamma_i \not\subset Interior(\Gamma_j)$ $i \neq j$. Iso-stress contours are not included in each other. (v) Γ_i is not self-intersecting.

These conditions must be kept in every iteration of the ESO algorithm. Figure 4 shows some non-trivial situations that must be handled to keep conditions (1-4) valid. Upper left figure displays invalid loci of iso-stress points. They are invalid because sudden interruptions (disappearances) of the path are not possible with continuous Φ functions. The cases in which the workpiece boundary interrupts the iso-stress locus and such a locus does not reappear elsewhere are invalid for the same reason. Intuitively, invalid paths are those that are not sufficient to split the workpiece into disjoint regions with $u(x, y) \neq u_0$. Regions of null area are not allowed.

Figure 4, upper right displays examples of valid iso-stress contours. They include cases of closed and open paths. The closed ones can be completed with the boundary of the workpiece. The lower right figure sketches the algorithms

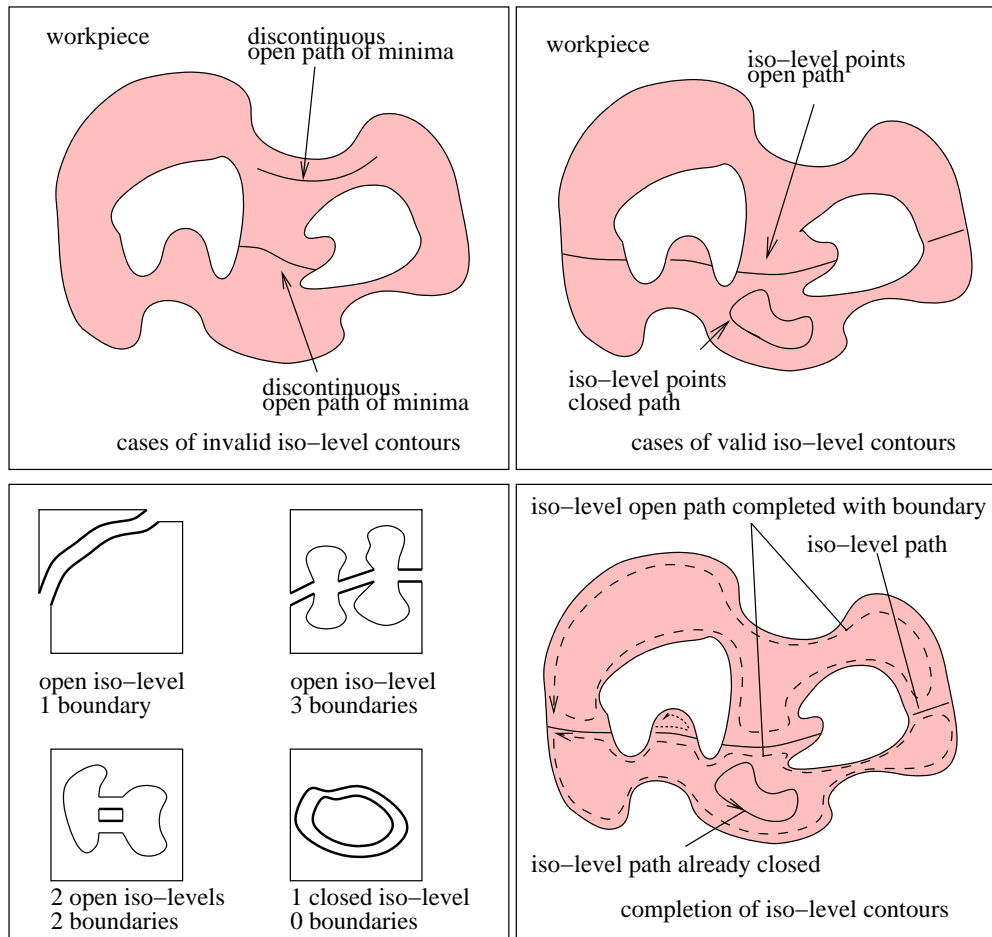


Figure 4: Cases of Workpiece split by Iso-stress contours

for contour identification and completion. The dashed line represents the closed contour that is obtained by completing the open loci of iso-stress points using the boundary of the workpiece. Notice that the regions so defined are topologically correct, and are ready to be subtracted from the original workpiece.

Figure 4 lower-left shows different (non-exhaustive) cases of the partition of the workpiece induced by the iso-stress paths. As mentioned before, a necessary condition for the iso-stress paths is that they must define regions with non-ambiguous, non-null interior/exterior.

2.3 Contour Algebra

At the i th iteration of the ESO algorithm, a level of stress σ_i is selected as threshold to trim the material that is at a lower level. The current workpiece at the beginning of the iteration is Ω_i . The k regions that are stressed at levels below the threshold are $\Omega_{i,1}, \Omega_{i,2}, \dots, \Omega_{i,k}$. Since the regions are bounded by topologically and geometrically correct paths, they will be identified with the

closed paths bounding them: Γ_i (the workpiece) and $\Gamma_{i,1}, \Gamma_{i,2}, \dots, \Gamma_{i,k}$. In this situation, the workpiece for the $i + 1$ th iteration is calculated as:

$$\Gamma_{i+1} = \Gamma_i - \bigcup_{j=1}^{j=k} \Gamma_{i,j} \quad (5)$$

where the $\Gamma_{i,j}$ are the boundaries of $\Omega_{i,j}$ regions that are identified as standing a stress level lower than the established threshold σ_i . These regions can be safely removed from the model. The operators in Equation (5) are the normal boolean and normalized set operators used in Computer Aided Geometric Design (CAGD). This investigation uses the 2D versions of them.

2.4 Mechanical Validation

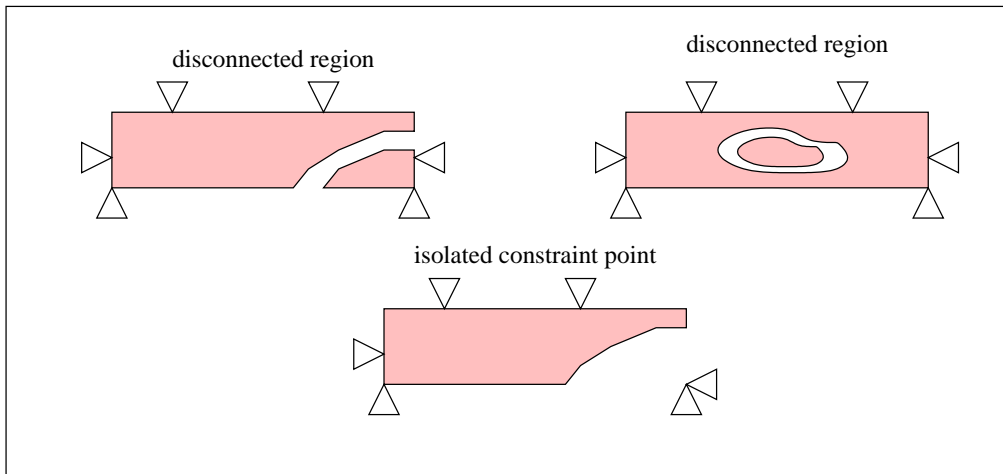


Figure 5: Mechanical Degeneracies from Material Removal

Condition (4) in subsection 2.2 is not a topological one. The 1-manifold formed by points $\{(x, y) | \Phi(x, y) = \Phi_0\}$ does not have to be connected and indeed iso-stress contours may appear within each other. However, such a situation generates a deficiency in mechanical constraints (see Figure 5), since it produces disconnected, statically unstable portions of the workpiece. The issue of automatic computation of sufficient kinematic constraints is outside the scope of this paper, and it is an open field of research in the areas of fixturing and grasping. For the present work, the existence of isolated, statically unstable regions was detected by testing: (i) inclusion of the closed paths corresponding to the same iso-stress in each other, and (ii) separate LUMPS of material (in the sense of solid modeling). This is not an exhaustive test, but impedes the existence of *bands* of removed material that would produce separate portions of workpiece. These portions may still be stable, given certain configurations of the constraining points. At the present, the elimination of separate regions

in non trivial cases (ii) is performed by the user. He/she determines, according to the product design conditions and static stability considerations, which connected parts of the piece are to be kept and which to be neglected. Notice that condition (i) above is detected by the algorithm.

3 RESULTS

Figure 6 shows different stages of the non-orthogonal ESO algorithm for a Michell type structure. Part (a) presents the workpiece at the beginning of iteration. Part (b) corresponds to the 18th iteration, (c) to the 43th and (d) to the 84th iteration. The mesh size was 300 elements. The total computing time was 4.9 minutes on a Pentium 500 MHz processor. Table 1 shows a comparison of the present approach (ISO ESO) with classic ESO and FG ESO. Standard ESO and FG-ESO results were obtained from Kim et al and were measured using a Pentium 133 MHz processor [10]. The mesh size in this case was 50×50 . ISO-ESO time was measured with a Pentium 500 MHz computer and scaled to a Pentium 133 MHz in order to compare the results.

Due to the differences in FEA solvers and the way material is removed, notice that classic ESO introduces stress concentration regions because of the jagged surface, the path of the three methods differs and therefore reduction of the volume to 40 % of the initial volume is reached at different number of iterations, table 1.

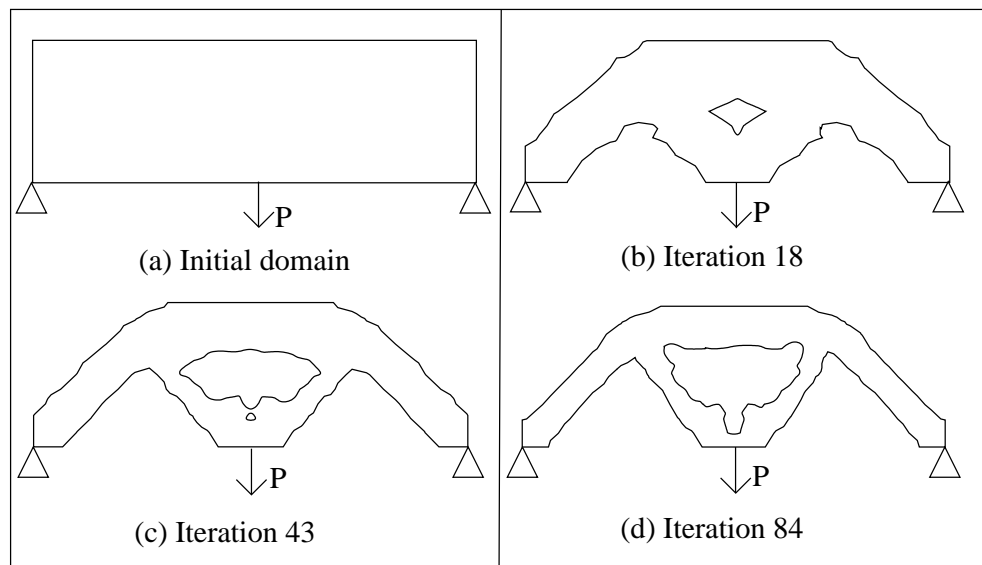


Figure 6: Workpiece Evolution from Non-Orthogonal Iso-stress Segment Calculation

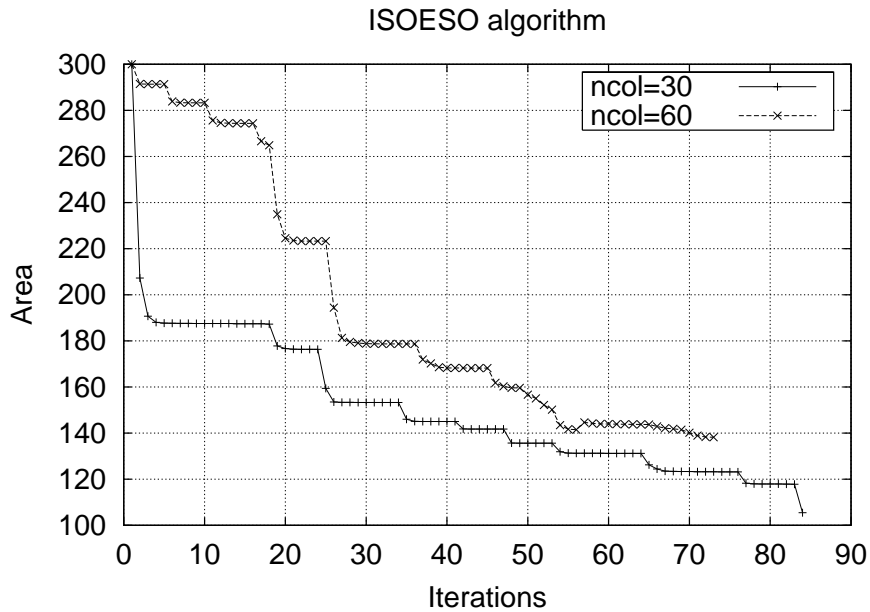


Figure 7: Evolutionary History of volume

	Standard ESO	FG ESO	Iso ESO
Volume reduction	40.12 %	39.9 %	35.0 %
Number of Iterations	838	188	84
Solution Time	22:55:30	2:22:52	0:30:00

Table 1: Comparison of Michell type structure optimisation process by different ESO methods

4 CONCLUSIONS

This work has presented a variation of the ESO algorithm based on iso-stress-driven material removal instead of the element-based material removal criteria used by classic ESO. Stress distribution is obtained with the FG method by using a re-analysis technique thus reducing the total computational time. Preliminary results showed significant savings on time when compared with classic ESO and FG ESO. The present approach keeps the B-rep of the geometry/topology at every step of the evolution process and therefore a more feasible and manufacture optimised topologies. It is also noted that the topologies produced by this method do not contain checkerboard patterns.

REFERENCES

- [1] GARCÍA MJ AND STEVEN GP. Fixed grid finite elements in elasticity problems. Engineering Computations, Vol 16, No. 2, pp 145–164, 1999.
- [2] GARCÍA MJ AND STEVEN GP. Displacement error for fixed grid finite fea elasticity problems. In Third Colombian Congress in Finite Elements, Medellin, October 1996.

- [3] XIE YM AND STEVEN GP. A simple evolutionary procedure for structural optimization. Computers and Structures, Vol 49, No. 5, pp 885–896, 1993.
- [4] XIE Y AND STEVEN G. Evolutionary Structural Optimisation. Springer, Melbourne, 1997.
- [5] XIE YM AND STEVEN GP. Optimal design of multiple load case structures using an evolutionary procedure. Engineering Computations, Vol 11, pp 295–302, 1994.
- [6] QUERIN O, STEVEN G, AND XIE Y. Topology optimisation of structures with material and geometric non-linearities. In Sixth AIAA/USAF/NASA/ISSMO Symposium on Multidisciplinary Analysis and Optimization, Washington, pp 1812–1818, 1996.
- [7] ZHAO C, G.P. S, AND XIE Y. Evolutionary natural frequency optimization of thin plate bending vibration problems. Journal of Structural Optimization, , No. 11, pp 244–251, 1996.
- [8] MANICKARAJAH D, XIE Y, AND STEVEN G. Structural Stability and Design, chapter A Simple Method for the Optimisation of Columns, Frames and Plates Against Buckling, pp 175–180. A. A. Balkema, Rotterdam.
- [9] QUERIN O, STEVEN G, AND XIE Y. Evolutionary structural optimisation (eso) using a bidirectional algorithm. Engineering Computations, Vol 15, No. 8, pp 1031–1048, 1998.
- [10] KIM H, GARCÍA MJ, QUERIN OM, STEVEN GP, AND XIE YM. Fixed grid finite element analysis in evolutionary structural optimisation. Engineering Computations, Vol 17, No. 4, pp 427–439, 2000.
- [11] DÍAZ A AND SIGMUND O. Checkerboard patterns in layout optimization. Structural Optimization, Vol 10, pp 40–45, 1995.
- [12] JOG CS AND HABER RB. Stability of finite element models for distributed-parameter optimization and topology design. Computer Methods in Applied Mechanics and Engineering, Vol 130, pp 203–226, 1996.